

Localization and slow-thermalization in a cluster spin model

Yoshihito Kuno¹, Takahiro Orito², and Ikuo Ichinose³

¹*Department of Physics, Graduate School of Science,
Tsukuba University, Tsukuba, Ibaraki 305-8571, Japan*

²*Graduate School of Advanced Science and Engineering, Hiroshima University, 739-8530, Japan and*

³*Department of Applied Physics, Nagoya Institute of Technology, Nagoya, 466-8555, Japan*

(Dated: October 13, 2021)

New cluster spin model with interactions and disorder is studied. In certain type of interactions, we find an extensive number of local integrals of motion (LIOMs), which are a modified version of the stabilizers, but not dressed spins. These LIOMs can be defined for any strength of the interactions and disorder. Hence, even under the presence of interactions, integrability is held, and all eigenvalues are labeled by these LIOMs. Localization is, then, expected to occur. We numerically investigate this expectation in detail. In particular, ergodicity breaking dynamics is demonstrated where symmetry-protected-topological order also preserves for specific initial states.

Introduction.— The notions of localization and thermalization are deeply related [1, 2]. In a closed system separated from environment, if states are localized, the system does not thermalize. This character persists even in interacting many-body systems, phenomenon called many-body-localization (MBL) [3, 4]. Such non- or slow-thermalization dynamics is a novel example for the breaking of the eigenstate thermalization hypothesis [1, 5]. Also, weak localization and weak ergodicity breaking in some specific models such as quantum scar states are now getting a lot of attention [6–18]. What types of models exhibit localization or MBL phenomena, i.e., non- or slow-thermalization dynamics, and what constraints induce them are significant questions. To answer them, a key concept is an extensive number of local integrals of motions (LIOMs) [19–22]. Investigating the LIOMs in specific models is important and useful to scrutinize localization phenomena from the general perspective. Constructing some classification schema of localization from a bottom-up approach by the study on various concrete examples is an important subject [16].

In this Letter, we study a specific example of systems, in which LIOMs are obtained explicitly. The LIOMs are compact support in the system with certain interactions and disorder, and the system exhibits localization phenomena in its dynamics. Model describing this system is an extended version of the cluster model [23–26], which includes interactions and disorder. In the pure cluster model, the model exhibits localization phenomena with symmetry-protected-topological (SPT) order [27–38]. For the extended version of the cluster model, we find localization phenomena such as slow-thermalization analog to Anderson localization. The extensive number of LIOMs are modified counterparts of the stabilizers in the pure cluster model, and they label all eigenstates of the interacting and disordered Hamiltonian. The compact support of the LIOMs is related to the fact that the interactions only locally mix many-body states. Expected localization phenomena in the model including ergodicity breaking are numerically demonstrated. We,

furthermore, investigate how localization and the SPT order are destroyed as an additional interaction is added, although they are quite stable regardless of the strength of the original interactions and disorder.

Model.— In this Letter, we work on an extended version of the cluster spin model with interactions and disorder, the original model of which was studied in Ref. [23–26],

$$H = \sum_{\ell=0}^{L/2-1} [J_{2\ell}K_{2\ell} + J_{2\ell+1}K_{2\ell+1}] + H_{\text{int}} \quad (1)$$

$$H_{\text{int}} = \sum_{\ell=0}^{L/2-1} gV_{\ell}, \quad (2)$$

where $K_j = \sigma_{j-1}^z \sigma_j^x \sigma_{j+1}^z$ is a stabilizer operator composed of Pauli matrices, $V_{\ell} = N_{\ell-1}[K_{2\ell}^+ K_{2\ell+1}^- + K_{2\ell}^- K_{2\ell+1}^+]$, $N_{\ell} = K_{2\ell} + K_{2\ell+1}$ and $K_j^{\pm} = \frac{1}{2}(\sigma_j^z \mp i\sigma_{j-1}^z \sigma_j^x \sigma_{j+1}^z)$. K_j^{\pm} is a raising and lowering operator for cluster state [17], J_j is site-dependent potential of the stabilizer K_j and g is strength of the interactions. The stabilizer K_j is a dressed spin, which satisfies $K_j^2 = 1$ and $\text{SU}(2)$ -spin algebra, $[K_j, K_j^{\pm}] = \pm 2K_j$. The Hamiltonian H has $\mathbb{Z}_2 \times \mathbb{Z}_2^T$ symmetry, which is composed of the global spin flip $\prod_{j=0}^{L-1} \sigma_j^x$ and the complex conjugation (time-reversal operation) [39–41]. For $g = 0$, the set of the stabilizer $\{K_j\}$ becomes an extensive number of LIOMs since $[H_{g=0}, K_j] = 0$ and $[K_j, K_{j'}] = 0$ for any j and j' . When the site-dependent coupling J_j ($j = 0, 1, \dots, L-1$) is randomly valued, the system exhibits localization with short-range entanglement coming from the cluster state, where every eigenstate is uniquely labeled by the set of eigenvalues of the LIOMs, $K_j = \pm 1$. This localization is stable against perturbations (interactions) preserving the symmetry, namely, topological MBL, which has been studied extensively [28–38]. In this Letter, we focus on $g \neq 0$ and a type of disorder such as $J_{2\ell} = -J_{2\ell+1} = \lambda_{\ell}$, where λ_{ℓ} 's are uniformly-distributed random variables, $\lambda_{\ell} \in [-W, W]$. In this case, the system has modified LIOMs as we show shortly.

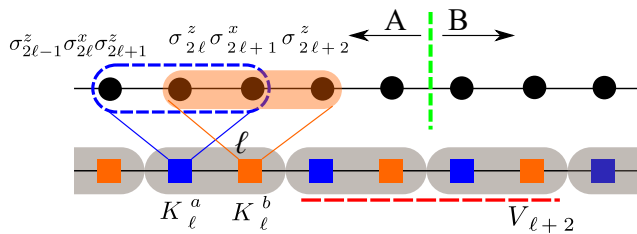


FIG. 1. Schematic figure of the Model, Eq. (3). The upper chain is the original spin-lattice. The original spin-lattice is mapped onto the cluster-basis lattice in the lower chain. The green vertical dashed line represents the entanglement cut for a pair of subsystems in the calculation of the EE.

Modified local integrals of motion.— Under the disorder $\{\lambda_\ell\}$, the target cluster model is rewritten as

$$H = H_0 + H_{\text{int}}, \quad H_0 = \sum_{\ell=0}^{L/2-1} \lambda_\ell [K_\ell^a - K_\ell^b], \quad (3)$$

where we have introduced unit-cell including two sites 2ℓ and $2\ell+1$, and “a” and “b” indices for even and odd sites in the unit-cell. The operators $K_{2\ell(2\ell+1)}$ are related as $K_\ell^{a(b)}$. The schematic lattice structure is shown in Fig. 1. Similar structure to $K_\ell^{a(b)}$ was used in other lattice models, e.g., compact localized states [42–44].

By following our previous study on the Creutz ladder [43], we find that there are operators commutative with the total Hamiltonian H , which are given by

$$\tilde{K}_\ell^a = K_\ell^a + \frac{g}{2\lambda_\ell} V_\ell, \quad \tilde{K}_\ell^b = K_\ell^b - \frac{g}{2\lambda_\ell} V_\ell, \quad (4)$$

and $H = \sum_{\ell=0}^{L/2-1} \lambda_\ell [\tilde{K}_\ell^a - \tilde{K}_\ell^b]$. These operators are compact-support form and satisfy $[\tilde{K}_\ell^a, \tilde{K}_{\ell'}^{a(b)}] = 0$ for any ℓ and ℓ' , $[H, \tilde{K}_\ell^{a(b)}] = 0$. That is, these operators are LIOMs, which are a modified version of the original stabilizer K_j . Also, note that the LIOMs, $\tilde{K}_\ell^{a(b)}$, can be defined for any disorder realizations and interaction strength, $\{\lambda_\ell\}$ and g , whereas $(\tilde{K}_\ell^{a(b)})^2 \neq 1$, that is, the eigenvalues of $\tilde{K}_\ell^{a(b)}$ are not a discrete value ± 1 , but fractional in general, depending on the values of g and λ_ℓ . Hence, $\tilde{K}_\ell^{a(b)}|\psi_k\rangle = I_{a(b),\ell}^k|\psi_k\rangle$, where $I_{a(b),\ell}^k \in \mathbb{R}$ and $|\psi_k\rangle$ is k -th eigenstate of H . [We use the ascendant order for the energy eigenstates.] Here, we remark that we can extend systems to the one with long-range interactions with modified LIOMs *beyond compact support*, which we comment on in conclusion.

In the following, we show how the LIOMs label all eigenstates. Since extensive number of the LIOMs $[\tilde{K}_\ell^{a(b)}]$ exist, the system can exhibit localization nature, somewhat analog to Anderson localization of cluster-spin basis. Furthermore, as characteristic dynamical properties, non- or slow-thermalized dynamics appears [5].

Study of small system.— We study a small system with $L = 6$ to see how the system is affected by the interactions, how the eigenstates are characterized by LIOMs and how localization properties emerge.

In this small system, we first focus on the ℓ -th unit-cell in the stabilizer lattice in Fig. 1 and investigate the eigenvalues and eigenstates of the non-interacting Hamiltonian H_0 . For any λ_ℓ , there are three energy levels, $\epsilon = -2\lambda_\ell, 0, 2\lambda_\ell$, where their eigenstates are given by $|\bar{1}\bar{1}\rangle_\ell$ for $\epsilon = -2\lambda_j$, two orthogonal linear-superposed states denoted by $\alpha|11\rangle_\ell + \beta|\bar{1}\bar{1}\rangle_\ell$ for $\epsilon = 0$, and $|\bar{1}\bar{1}\rangle$ for $\epsilon = 2\lambda_j$, where we have introduced a notation such as $|1\bar{1}\rangle_\ell = K_\ell^{a+} K_\ell^{b-} |\uparrow\rangle_\ell$ ($|\uparrow\rangle_\ell$ is all up states around ℓ unit-cells in the original spin lattice). Therefore, $K_\ell^a|1\bar{1}\rangle_\ell = |1\bar{1}\rangle_\ell$, $K_\ell^b|1\bar{1}\rangle_\ell = -|1\bar{1}\rangle_\ell$. The presence of an arbitrary linear-superposed state at zero energy of H_0 prevents unique-labeling of eigenstates by the LIOMs. A pair of the doubly degenerate states can be chosen arbitrarily as long as they are orthogonal to each other. Thus, we take $|\bar{1}\bar{1}\rangle_\ell$ and $|11\rangle_\ell$ as a pair of orthogonal eigenstates with zero energy of H_0 . To impose this choice in practical calculations, we introduce very small random potential, $\sum_\ell \delta h_\ell [K_\ell^a + K_\ell^b]$ with $\delta h_\ell \in [-\delta h, \delta h]$, $\delta h = 0.5 \times 10^{-5}W$. This ‘fictitious’ disorder gives little effect to the entire physics, especially, to the dynamical behavior of the system. Under this manipulation, “cluster-basis” eigenstates of H_0 are described as $|\psi(\{a_\ell\}, \{b_\ell\})\rangle = \prod_{\ell=0}^{L/2} K_\ell^{a_\ell} K_\ell^{b_\ell} |\uparrow\rangle$ [17], where L is an even number, the sets of $\{a_\ell\}, \{b_\ell\}$ are a sequence of + and – labels and $|\uparrow\rangle$ is a L -site ferromagnetic state with all spins up in the original spin basis.

Removing the degeneracy of the zero-energy state of H_0 in single unit-cell as explained in the above, we study effects of the interaction H_{int} on the cluster-basis eigenstates of H_0 . Here, an interaction term V_ℓ acts over two unit-cells as shown in the lower lattice in Fig. 1. Only four cluster-basis states on the $\ell-1$ and ℓ unit-cells are changed: (i) $|11\rangle_{\ell-1}|1\bar{1}\rangle_\ell$, (ii) $|11\rangle_{\ell-1}|\bar{1}\bar{1}\rangle_\ell$, (iii) $|\bar{1}\bar{1}\rangle_{\ell-1}|1\bar{1}\rangle_\ell$, (iv) $|\bar{1}\bar{1}\rangle_{\ell-1}|\bar{1}\bar{1}\rangle_\ell$. The interaction V_ℓ mixes (i) and (ii) ((iii) and (iv)), and creates a mixing state of $|1\bar{1}\rangle_\ell$ and $|\bar{1}\bar{1}\rangle_\ell$. For the other cluster-basis states on the two unit-cells are a null state of V_ℓ .

From the above observation about the action of V_ℓ , characteristic eigenstates for the $L = 6$ interacting system of H are obtained straightforwardly. As an examples, $|\psi_{1,\pm}^{L=6}\rangle = |11\rangle_0|s^\pm\rangle_1|11\rangle_2$ where $|s^\pm\rangle_1 = \alpha_1^\pm|1\bar{1}\rangle_1 + \alpha_2^\pm|\bar{1}\bar{1}\rangle_1$ and $(\alpha_1^\pm, \alpha_2^\pm) = [4g^2 + (2\lambda_1 - \epsilon_1^\pm)^2]^{-1/2}(2g, \epsilon_1^\pm - 2\lambda_1)$ with $\epsilon_1^\pm = \pm 2[\lambda_\ell^2 + g^2]^{1/2}$. The state, $|\psi_{1,\pm}^{L=6}\rangle$, is an eigenstate for all LIOMs, $\tilde{K}_\ell^{a(b)}$, with integer or fractional eigenvalues, e.g., $\tilde{K}_1^a|\psi_{1,\pm}^{L=6}\rangle = \frac{\epsilon_1^\pm}{2\lambda_1}|\psi_{1,\pm}^{L=6}\rangle$ and $\tilde{K}_1^b|\psi_{1,\pm}^{L=6}\rangle = -\frac{\epsilon_1^\pm}{2\lambda_1}|\psi_{1,\pm}^{L=6}\rangle$. From this observation of $|\psi_{1,\pm}^{L=6}\rangle$, certain cluster-basis eigenstates of H_0 , $|\psi(\{a_\ell\}, \{b_\ell\})\rangle$ are mixed by the interactions H_{int} , however, the mixing is local and only small numbers of

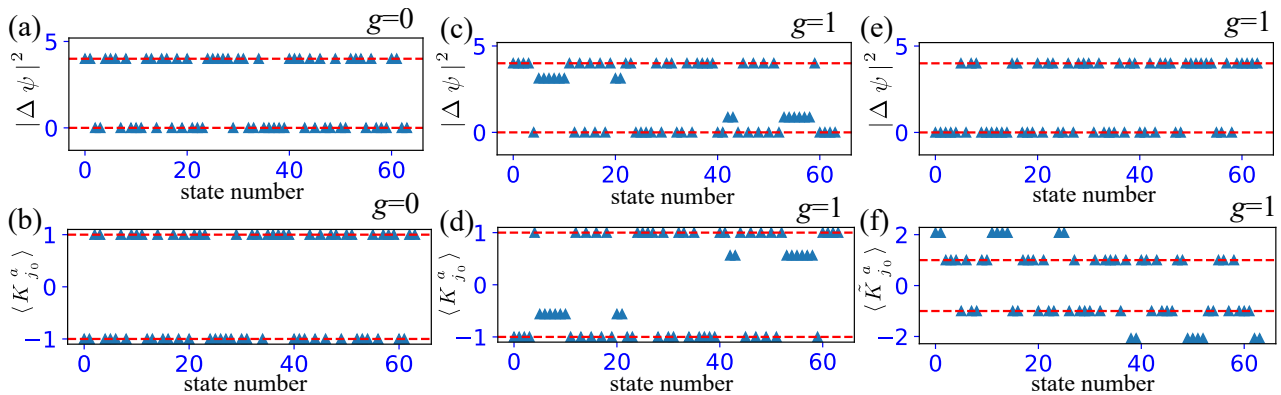


FIG. 2. Identification of eigenstates and their LIOM-eigenvalues for three unit-cell system ($L = 6$). (a) $|\Delta\psi_k|^2$ for each eigenstate for $g = 0$ case. (b) Each eigenvalue of $K_{\ell_0}^a$ for $g = 0$ case. (c) $|\Delta\psi_k|^2$ for each eigenstate for finite g in terms of $K_{\ell_0}^a$. (d) Each eigenvalue $\langle\psi_k|K_{\ell_0}^a|\psi_k\rangle$ for finite g case. (e) $|\Delta\psi_k|^2$ for each eigenstate for finite g in terms of $\tilde{K}_{\ell_0}^a$. (f) Each eigenvalue of $\tilde{K}_{\ell_0}^a$ for finite g case. All results are obtained for a single-shot disorder. Energy eigenstates are numbered in the ascendant order.

cluster-basis eigenstates are affected. These observations indicate that global hybridization does not occur by the interactions H_{int} due to the presence of the extensive number of the modified LIOMs, $\tilde{K}_{\ell}^{a(b)}$. [We give observation of the general structure of the Hilbert space for the L -site system in [45].]

Following the above analytical observation, we numerically study the LIOMs in the $L = 6$ system [46]. [We employ the periodic boundary condition.] We observe whether the operators $\{\tilde{K}_j^a\}$ operate as the LIOMs for all eigenstates, i.e., all energy eigenstates are the eigenstates of the LIOMs. To this end, we first examine whether the resulting states obtained by acting $\tilde{K}_{\ell_0}^a$ on energy eigenstates are proportional to the original ones. Numerically, for k -th eigenstate $|\psi_k\rangle$, we define $|\tilde{\psi}_k\rangle \equiv \tilde{K}_{\ell_0}^a|\psi_k\rangle/\sqrt{|\tilde{K}_{\ell_0}^a|\psi_k\rangle}$ and calculate $|\Delta\psi_k|^2 = \|\psi_k - |\tilde{\psi}_k\rangle\|^2$. Then, if $|\Delta\psi_k|^2 = 0$ or 4, $|\psi_k\rangle$ is also an eigenstate of $\tilde{K}_{\ell_0}^a$ with the eigenvalue, $I_{a,\ell_0}^k = \langle\psi_k|\tilde{K}_{\ell_0}^a|\psi_k\rangle$. Here, we set $\ell_0 = 1$ for the practical calculation.

We show numerical results. For the $g = 0$ case, all eigenstates for single-shot disorder realization are labeled by the original stabilizers, $\{K_{\ell}^{a(b)}\}$. Each $|\Delta\psi_k|^2$ takes 0 or 4 and the LIOMs' eigenvalues are $I_{a,1}^k = \pm 1$ as shown in Figs. 2 (a) and (b). For the $g = 1$ case, we first operate the original $\{K_{\ell}^{a(b)}\}$ to energy eigenstates for $g = 1$ to see that $\{K_{\ell}^{a(b)}\}$ are *not* genuine LIOMs. As shown in Figs. 2 (c) and (d), some of $|\Delta\psi_k|^2$ deviate from 0/4 and $\langle\psi_k|\tilde{K}_{\ell_0}^a|\psi_k\rangle$ deviate from ± 1 . On the other hand for the operation of $\tilde{K}_{\ell_0}^{a(b)}$, $|\Delta\psi_k|^2$ takes 0 or 4, that is, $\tilde{K}_{\ell_0}^a$ is a genuine LIOM with eigenvalues $\{I_{a,1}^k\}$, where some of $I_{a,1}^k$ takes a disorder-dependent fractional value. Also, note that the interactions H_{int} has some large kernel space,

$H_{\text{int}}|\psi_k\rangle = 0$, which means that a substantial number of eigenstates still have $\tilde{K}_{\ell}^a = K_{\ell}^a$ with eigenvalues ± 1 .

From the above study on the small system, we found that the modified LIOMs, $\{\tilde{K}_{\ell}^{a(b)}\}$, indeed label all energy eigenstates. We expect that this holds for the system with larger sizes. Also, the interaction H_{int} mixes only a small number of local cluster-basis eigenstates of H_0 . This fact implies that the interacting model in the present work exhibits localization phenomena analogous to Anderson localization. In what follows, to elucidate it we examine the dynamics of the system.

Numerical demonstration of localization dynamics.— We numerically demonstrate localization phenomena for larger systems. In what follows, we remove the ‘fictitious’ disorder, $\delta h_{\ell} = 0$. The interaction H_{int} affects to the system locally, mixing a few cluster-basis eigenstates, and also has large kernel space, $H_{\text{int}}|\psi_k\rangle = 0$. From these facts and the existence of the extensive numbers of LIOMs, $\tilde{K}_{\ell}^{a(b)}$, we expect localization phenomena in the interacting system [H in Eq. (3)], especially, the quench dynamics that exhibits non- or slow-thermalization [5].

We observe Loschmidt echo (LE), given by $(\text{LE}) = |\langle\psi(t)|\psi(0)\rangle|^2$ where $|\psi(t)\rangle$ is the many-body wave function at time t , and the entanglement entropy (EE), defined as $S = -\text{Tr}[\rho_A \ln(\rho_A)]$ with A -subsystem reduced density matrix $\rho_A = \text{Tr}_B[\rho]$, where ρ is a density matrix of the entire system and the subsystem is set to $L/2(L/2 + 1)$ -site system for even (odd) L . For the practical calculation, A and B subsystems are set as shown in Fig. 1. In what follows, time is measured in units $[g/\hbar]$ and we set a random cluster-basis state (e.g., $|1\bar{1}1\bar{1}\bar{1}\dots\rangle$) as an initial state. In the quench dynamics, we average over 80 samples for the initial state and disorder realizations, $\{\lambda_{\ell}\}$.

Numerical results are displayed in Fig. 3. The LE re-

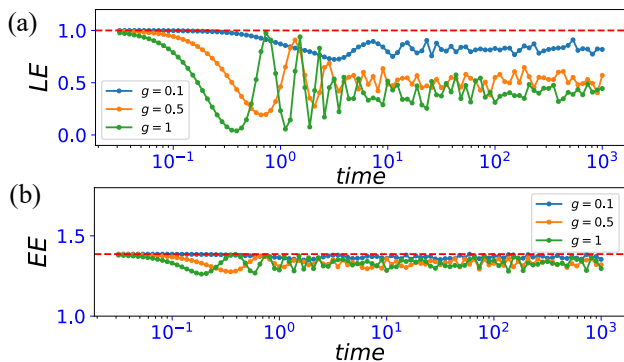


FIG. 3. Dynamics of LE [(a)] and EE [(b)]. We set $L = 12$ and averaged over 60 disorder realization for $W = 2$ and initial random cluster-basis state. The EE is quite stable, and its value is close to $2 \ln 2$ (corresponding to the value obtained by cut two clusters). We set $\delta h = 0$.

remains large finite values for a long period and the EE remains low-values around $2 \ln 2$ [47] as shown in Figs. 3 (a) and 3 (b) [48]. These behaviors retain for large g 's. The results of the LE in Fig. 3 (a) indicate that initial-state information is preserved, which indicates ergodicity breaking and also the behavior of EE implies all eigenstates of H remains to be low-entangled [45]. These numerical results indicate even for the cluster model with interactions H_{int} , genuine localization dynamics with short-range entanglement retains, which is similar to Anderson localization.

Effects of additional interactions: Many-body localization dynamics.— We add an Ising interaction to the system, $V_{zz} = \sum_{j=0}^{L-1} v_{zz} \sigma_j^z \sigma_{j+1}^z$, and observe how the localization nature of the model [Eq. (3)] changes. The interaction, V_{zz} , preserves the $\mathbb{Z}_2 \times \mathbb{Z}_2^T$ symmetry, and therefore, we expect that the SPT order persists even in the presence of V_{zz} . Obviously for finite v_{zz} , the operator $\tilde{K}_\ell^{a(b)}$ is no longer exact LIOMs, but some emergent LIOMs might appear, as suggested in [28].

We observe that the level-spacing analysis for the system with finite v_{zz} exhibits localization properties. [See [45]]. Then, we numerically investigate the quench dynamics of the model with finite g and v_{zz} , where we set the cluster-basis Neel state $|\uparrow\downarrow\uparrow\downarrow\uparrow\downarrow\cdots\rangle$ as an initial state and observe the LE, EE and a loop order (LO) defined by $(\text{LO}) = \langle \Psi(t) | \hat{L} | \Psi(t) \rangle$ with $\hat{L} = \prod_{\ell=0}^{L/2-1} K_\ell^a$ [49]. The LO diagnoses the presence of SPT order.

Numerical results are shown in Fig. 4, where we set $g = 1$. For small v_{zz} , the value of the LE remains finite [Fig. 4 (a)], the increase of the EE is much suppressed [Fig. 4 (b)] and also the value of the LO remains finite [Fig. 4 (c)] for a long period. Obviously, these are MBL behavior with SPT order. For larger v_{zz} , localization tendency is weakened, i.e., the increase of the EE is enhanced with logarithmic growth and saturates with larger

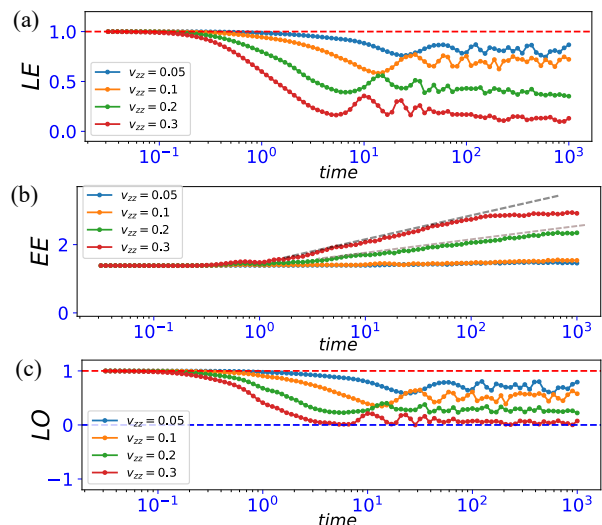


FIG. 4. Dynamics of LE [(a)], EE [(b)] and LO [(c)]. We set $L = 12$, $W = 2$, $g = 1$ and $\delta h = 0$ and averaged over 40 disorder realizations.

values, approaching to the Page value [50], $(L \log 2 - 1)/2$. Correspondingly, the values of the LE and LO also are decreasing, thermalization tendency is enhanced and the SPT order is fading away. We furthermore investigate the behavior of a modified LO order described by \tilde{K}_ℓ^a , and find that SPT order again survives for short periods, as the details are shown in [45].

Conclusion.— We showed that a specific type of interacting cluster model with disorder exhibits genuine MBL. LIOMs modified from the stabilizer operators were found for arbitrary strength of interactions and disorder. We showed that the LIOMs label all energy eigenstate. The locality of the LIOMs and extensive number of them imply localization phenomena analogous to Anderson localization. We numerically demonstrated that the quench dynamics of the system shows non-thermalized dynamics (ergodicity breaking dynamics), characteristic of the localization phenomena with SPT order. Further, non-thermalized dynamics is stable against weak interactions. The localization tendency characterized by the LIOMs $[\tilde{K}_\ell^{a(b)}]$ survives in the presence of the Ising interactions, V_{zz} .

Finally, we comment that another type of the LIOMs can be defined, which have not compact but a long-tail support [51]. The study of such modified LIOM system is an interesting future topic.

The work is supported by JSPS KAKEN-HI Grant Number JP21K13849 (Y.K.).

-
- [1] R. Nandkishore, and D. A. Huse, Annual Review of Condensed Matter Physics **6**, 15 (2015).
- [2] D. A. Abanin, E. Altman, I. Bloch, and M. Serbyn, Rev. Mod. Phys. **91**, 021001 (2019).
- [3] D. M. Basko, I. L. Aleiner, and B. L. Altshuler, Ann. Phys. **321**, 1126 (2006).
- [4] J. H. Bardarson, F. Pollmann, and J. E. Moore, Phys. Rev. Lett. **109**, 017202 (2012).
- [5] M. Rigol, V. Dunjko, V. Yurovsky, and M. Olshanii, Phys. Rev. Lett. **98**, 050405 (2007).
- [6] H. Bernien, S. Schwartz, A. Keesling, H. Levine, A. Omran, H. Pichler, S. Choi, A. S. Zibrov, M. Endres, M. Greiner, V. Vuletić, and M. D. Lukin, Nature **551**, 579 (2017).
- [7] C. J. Turner, A. A. Michailidis, D. A. Abanin, M. Serbyn, and Z. Papić, Nat. Phys. **14**, 745 (2018).
- [8] S. Choi, C. J. Turner, H. Pichler, W. W. Ho, A. A. Michailidis, Z. Papić, M. Serbyn, M. D. Lukin, and D. A. Abanin, Phys. Rev. Lett. **122**, 220603 (2019).
- [9] W. W. Ho, S. Choi, H. Pichler, and M. D. Lukin, Phys. Rev. Lett. **122**, 040603 (2019).
- [10] T. Iadecola and M. Schecter, Phys. Rev. B **101**, 024306 (2020).
- [11] D. Bluvstein, A. Omran, H. Levine, A. Keesling, G. Semeghini, S. Ebadi, T. T. Wang, A. A. Michailidis, N. Maskara, W. W. Ho, S. Choi, M. Serbyn, M. Greiner, V. Vuletic, and M. D. Lukin, arXiv:2012.12276 [quant-ph] (2020).
- [12] P. A. McClarty, M. Haque, A. Sen, and J. Richter, Phys. Rev. B **102**, 224303 (2020).
- [13] N. Shibata, N. Yoshioka, and H. Katsura, Phys. Rev. Lett. **124**, 180604 (2020).
- [14] K. Lee, R. Melendrez, A. Pal, and H. J. Changlani, Phys. Rev. B **101**, 241111 (2020).
- [15] Y. Kuno, T. Mizoguchi, Y. Hatsugai, Phys. Rev. B **102**, 241115 (R) (2020).
- [16] M. Serbyn, D. A. Abanin and Z. Papić, Nat. Phys. **17**, 675 (2021).
- [17] J. Jeyaretnam, J. Richter, and A. Pal, Phys. Rev. B **104**, 014424 (2021).
- [18] Y. Kuno, T. Mizoguchi, Y. Hatsugai, Phys. Rev. B **104**, 085130 (2021).
- [19] M. Serbyn, Z. Papić, and D. A. Abanin, Phys. Rev. Lett. **111**, 127201 (2013).
- [20] D.A. Huse, R. Nandkishore, and V. Oganesyan, Phys. Rev. B **90**, 174202 (2014).
- [21] J. Z. Imbrie, J. Stat. Phys **163**, 998 (2016).
- [22] J.Z. Imbrie, V. Ros, and A. Scardicchio, Ann. Phys. (Berlin) **529**, 7, 1600278 (2017).
- [23] H. J. Briegel and R. Raussendorf, Phys. Rev. Lett. **86**, 910 (2001).
- [24] J. K. Pachos and M.B. Plenio, Phys. Rev. Lett. **93**, 056402 (2004).
- [25] W. Son, L. Amico, R. Fazio, A. Hamma, S. Pascazio, and V. Vedral, Europhys. Lett. **95**, 50001 (2011).
- [26] P. Smacchia, L. Amico, P. Facchi, R. Fazio, G. Florio, S. Pascazio, and V. Vedral, Phys. Rev. A **84**, 022304 (2011).
- [27] B. Bauer and C. Nayak, J. Stat. Mech. Theory Exp. **P09005** (2013).
- [28] Y. Bahri, R. Vosk, E. Altman, and A. Vishwanath, Nat. Commun. **6**, 7341 (2015).
- [29] R. Vasseur, A.J. Friedman, S.A. Parameswaran, and A.C. Potter, Phys. Rev. B **93**, 134207 (2016).
- [30] S.A. Parameswaran and R. Vasseur, Reports Prog. Phys. **81**, 082501 (2018).
- [31] K.S.C. Decker, D.M. Kennes, J. Eisert, and C. Karrasch, Phys. Rev. B **101**, 014208 (2020).
- [32] Y. Kuno, Phys. Rev. Research **1**, 032026(R) (2019).
- [33] T. B. Wahl and B. Béri, Phys. Rev. Research **2**, 033099 (2020).
- [34] A. Chan and T. B. Wahl, J. Phys.: Cond. Mat. **32**, 305601 (2020).
- [35] J. Li, A. Chan, and T. B. Wahl, Phys. Rev. B **102**, 014205 (2020).
- [36] J. Kemp, N. Y. Yao, and C. R. Laumann, Phys. Rev. Lett. **125**, 200506 (2020).
- [37] R. Sahay, F. Machado, B. Ye, C. R. Laumann, and N. Y. Yao, Phys. Rev. Lett. **126**, 100604 (2021).
- [38] C. M. Duque, H. Y. Hu, Y. Z. You, V. Khemani, R. Verresen, and R. Vasseur, Phys. Rev. B **103**, L100207 (2021).
- [39] R. Verresen, R. Moessner, and F. Pollmann, Phys. Rev. B **96** 101103 (2017).
- [40] R. Verresen, N. G. Jones, and F. Pollmann, Phys. Rev. Lett. **120** 057001 (2018).
- [41] A. Smith, B. Jobst, A.G. Green, and F. Pollmann, arXiv:1910.05351 (2020).
- [42] Y. Kuno, T. Orito, and I. Ichinose, New J. Phys. **22**, 013032 (2020).
- [43] T. Orito, Y. Kuno, and I. Ichinose, Phys. Rev. B **101**, 224308 (2020).
- [44] T. Orito, Y. Kuno, and I. Ichinose, Phys. Rev. B **104**, 094202 (2021).
- [45] See supplemental material: (I) Structure of Hilbert space. (II) The dependence of the fictitious disorder (III) System size dependence of the LE. (IV) Level spacing analysis for finite v_{zz} . (V) Calculations of a modified LO.
- [46] We employed the Quspin solver for all numerical calculations: P. Weinberg and M. Bukov, SciPost Phys. **7**, 20 (2019); **2**, 003 (2017).
- [47] This value of EE corresponds to the value when the two cluster states are cut.
- [48] Additional numerical calculations for system size dependence and the dependence of the fictitious disorder are given in Supplemental material [45].
- [49] The operator LO is related to the string order parameter, which characterizes the bulk SPT order [25, 26].
- [50] D. N. Page, Phys. Rev. Lett. **71**, 1291 (1993).
- [51] If in the model of Eq.(3), we change H_{int} to $H'_{\text{int}} = \sum_{r \neq 0, \ell} V_{\ell}^r$, where $V_{\ell}^r \equiv g e^{-|r|} N_{\ell+r} (K_{\ell}^{a+} K_{\ell}^{b-} + K_{\ell}^{a-} K_{\ell}^{b+})$, another type of LIOMs can be constructed such as $L_{\ell}^a \equiv K_{\ell}^a + \frac{1}{2\lambda_{\ell}} \sum_{r \neq 0} V_{\ell}^r$ and $L_{\ell}^b \equiv K_{\ell}^b - \frac{1}{2\lambda_{\ell}} \sum_{r \neq 0} V_{\ell}^r$. These LIOMs are not compact but a long-tail support. Hence, this system may induce MBL phenomena, which poses a future work.
- [52] V. Oganesyan and D.A. Huse, Phys. Rev. B **75**, 155111 (2007).

SUPPLEMENTAL MATERIAL

I. Structure of Hilbert space under ‘fictitious’ disorder

For L -site system, where the total dimension of Hilbert space is given by $N_D = 2^L$, all eigenstates $|\psi_k\rangle$ for H of Eq.(3) in the main text with $g \neq 0$ under weak ‘fictitious’ disorder are classified into two classes since the interaction acts to only the following four states in two unit-cells: $|11\rangle_{\ell-1}|\bar{1}\bar{1}\rangle_{\ell}$, $|11\rangle_{\ell-1}|\bar{1}\bar{1}\rangle_{\ell}$, $|\bar{1}\bar{1}\rangle_{\ell-1}|\bar{1}\bar{1}\rangle_{\ell}$, and $|\bar{1}\bar{1}\rangle_{\ell-1}|\bar{1}\bar{1}\rangle_{\ell}$.

The first class is composed of eigenstates satisfying $H_{\text{int}}|\psi_k\rangle = g \sum_{\ell} V_{\ell}|\psi_k\rangle = 0$, that is, the eigenstate $|\psi_k\rangle$ is a null state for H_{int} . On the other hand, the second class is composed of the ones satisfying $H_{\text{int}}|\psi_k\rangle = v_k|\psi_k\rangle$, where v_k is finite real value. The above classification can be understood by observing how the interaction acts on the eigenstates of H_0 .

In N_D eigenstates of H , $2^{L/2+1}$ eigenstates are totally unaffected by the interaction, H_{int} . These eigenstates consist of the following two categories: (I) in the eigenstate, the state of each unit-cell is given by $|11\rangle_{\ell}$ or $|\bar{1}\bar{1}\rangle_{\ell}$ (total $2^{L/2}$ eigenstates). (II) in the eigenstate, the state of each unit-cell are given by $|1\bar{1}\rangle_{\ell}$ or $|\bar{1}1\rangle_{\ell}$ (total $2^{L/2}$ eigenstates). Needless to say, these total $2^{L/2+1} \equiv N_D^1$ eigenstates are eigenstates of H_0 .

On the other hand, the number of eigenstates of H with finite interaction energies is obtained by counting the number of eigenstates of H_0 affected by the interaction H_{int} . This number can be counted as follows: (a) We consider the eigenstate in which the state of each unit-cell is given by $|11\rangle_{\ell}$ or $|\bar{1}\bar{1}\rangle_{\ell}$ (total $2^{L/2}$ eigenstates). (b) For each eigenstate, select k unit-cells and change their states of the unit-cells to $|1\bar{1}\rangle_{\ell}$ or $|\bar{1}1\rangle_{\ell}$, where k takes from 1 to $L/2 - 1$. The total number of eigenstates obtained in this way is $\sum_{k=1}^{L/2-1} 2^{L/2-k} \binom{L/2}{k} 2^k = 4^{L/2} - 2^{L/2+1} \equiv N_D^2$, which are affected by the interaction H_{int} . These N_D^2 eigenstates are the second ones. In addition, the total sum of the eigenstates of the first and second class is $N_D^1 + N_D^2 = N_D$.

Furthermore, the interaction H_{int} mixes the eigenstates of the second class of H_0 , that is, N_D^2 eigenstates of H_0 . However, the mixing is small and local. That is, the Hamiltonian matrix of H based on the N_D^2 eigenstates becomes a block matrix with many small blocks. This implies that the obtained eigenstates of the Hamiltonian matrix H are low-entangled, where the deviation of the EE of one of the eigenstates of H_0 is small.

II. Effect of fictitious disorder δh_{ℓ}

To understand the structure of the eigenstate of the Hamiltonian H of Eq. (3) in the main text, we added very small ‘fictitious’ disorder δh_{ℓ} . We expect that such

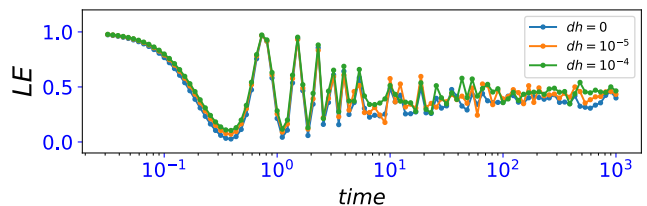


FIG. 5. Dependence on the strength of ‘fictitious’ disorder δh_{ℓ} of the LE with $\delta h_{\ell} \in [-\delta h, \delta h]$ (uniform distributed disorder). We set $L = 12$, $W = 2$, $g = 1$ and $v_{zz} = 0$. The initial state is a random cluster-basis state. We averaged over 80 disorder and random initial state samples.

a small δh_{ℓ} gives little effect to the localization nature of the system. As a concrete examination on this point, we observe the dependence on δh of the LE. The numerical estimation is shown in Fig. 5. The resultant dynamics of the LE is almost independent of the strength of δh where $\delta h \leq \mathcal{O}(10^{-4}g)$. From this fact, we expect that other physical observables in the system dynamics are not affected by the ‘fictitious’ disorder δh_{ℓ} .

III. System size dependence

We examine the system size dependence of the dynamics. In particular, we focus on the LE and calculated the LE for various system sizes. The result is shown in Fig. 6. From the left panel of Fig. 6, the system size dependence is small. All LEs remain at some finite value (~ 0.5) for a long period. We expect that the finite value of the LE also survives for larger system sizes as shown in the right panel of Fig. 6.

IV. Level spacing analysis for finite v_{zz}

To examine the presence of the localization tendency and the integrability of the system, we employed the level

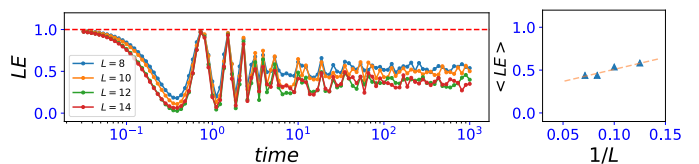


FIG. 6. Left panel: System size dependence of the LE for $L = 8, 10, 12$ and 14 . We set $W = 2$, $\delta h = 0$, $g = 1$, $v_{zz} = 0$. We averaged over disorder and random initial state samples, the numbers of the sample are 100, 80, 60 and 40 for $L = 8, 10, 12$ and 14 , respectively. Right panel: The system size dependence of the time average of the LE in from $t = 0.03$ to $t = 10^3$.

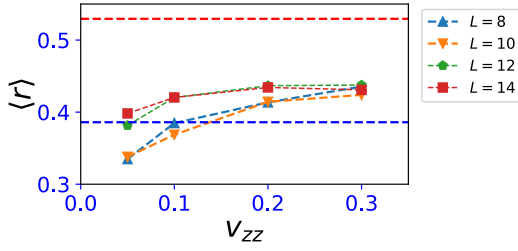


FIG. 7. Mean level spacing ratio $\langle r \rangle$ for the system with $L = 8 - 14$, $W = 2$, $g = 1$ and $\delta h_\ell = 0$. For small v_{zz} , $\langle r \rangle$ is close to the value of Poisson distribution. The numbers of the disorder sample are 100, 60, 40 and 30 for $L = 8, 10, 12$ and 14 , respectively. The red and blue dashed line are $\langle r \rangle = 0.5295$ and 0.386 , which are the values for the Wigner-Dyson and Poisson distributions, respectively.

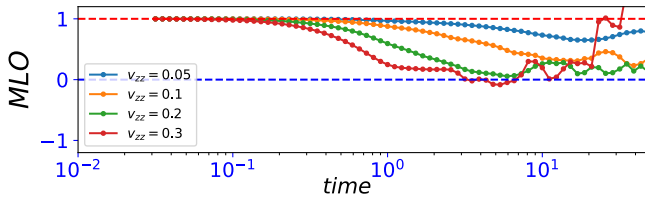


FIG. 8. The dynamical behavior of the MLO for various v_{zz} . We set $L = 12$, $W = 2$, $g = 1$ and $\delta h_\ell = 0$, and averaged over 40 disorder realizations for $\{\lambda_\ell\}$.

spacing analysis (LSA) for the system with finite v_{zz} [52]. We diagonalize the Hamiltonian $H + V_{zz}$, obtain all energy eigenvalues and calculate the level spacing ratio r_s

defined by $r_s = [\min(\delta^{(s)}, \delta^{(s+1)})] / [\max(\delta^{(s)}, \delta^{(s+1)})]$ for all s , where $\delta^{(s)} = E_{s+1} - E_s$ and $\{E_s\}$ is the set of energy eigenvalue in ascending order. Then, we calculate the mean level spacing ratio $\langle r \rangle$, which is obtained by averaging over r_s with employing all energy eigenvalues and also further averaging over disorder realizations for $\{\lambda_\ell\}$. The result for various system sizes and v_{zz} is shown in Fig. 7. For small v_{zz} , the remnant of degeneracy causes the mean value of the level spacing ratio to be smaller than that of the Poisson distribution, ~ 0.384 . However, for larger v_{zz} , the value is getting slightly larger than the Poisson distribution but stays near the value of the Poisson distribution. This indicates that the system is in a localized phase.

V. Calculation of an modified loop order

In the study of quench dynamics with finite g and v_{zz} , we further investigate the behavior of a modified loop order defined by $(\text{MLO}) = \langle \Psi(t) | \left[\prod_{\ell=0}^{L/2-1} \tilde{K}_\ell^a \right] | \Psi(t) \rangle$. Note that the operator depends on the set of disorder. We set the cluster-basis Neel state $|1\bar{1}1\bar{1}1\bar{1}\dots\rangle$ as an initial state, which has $(\text{MLO}) = 1(-1)$ for $L/2$ is even (odd). The dynamics of the MLO for various v_{zz} is shown in Fig. 8. For short-time, the values of the MLO remains the initial values. The initial value tends to decay after a long period of the time evolution, with large swings. This is due to the fact that state mixing with large LIOM eigenvalues occurs in the process of long time evolution.